UHV-ESR investigation of NO_2/Au(111)

1993 J. Phys.: Condens. Matter 5 5471

(http://iopscience.iop.org/0953-8984/5/31/011)

J. Phys.: Condens. Matter 5 (1993) 5471–5480. Printed in the UK

UHV–ESR investigation of NO_2/Au(111)

M Beckendorf, U J Katter, H Schlienz and H-J Freund

Lehrstuhl für Physikalische Chemie I, Ruhr-Universität Bochum, 44780 Bochum, Federal Republic of Germany

Received 21 December 1992, in final form 1 June 1993

Abstract. The adsorption of NO_2 on a clean Au(111) surface has been studied using electron spin resonance (ESR) and thermal programmed desorption (TPD). NO_2/Au(111) appears to be an appropriate system in which to detect an ESR signal, because it is known from the literature that NO_2 adsorbs as a molecule and is bonded through its oxygen atoms to the surface, while the spin is more localized at the nitrogen atom. In agreement with former results, no resonance of a paramagnetic monolayer on a clean single-crystal metal surface is observed. However, a well resolved spectrum from a multilayer has been detected. Orientation of the molecules in the multilayer has been studied via angle-dependent measurements in combination with computer simulation. Temperature-dependent measurements are used to investigate reactivity and molecular motion.

1. Introduction

There has been considerable interest in the investigation of paramagnetic adsorbates on solid surfaces. With electron spin resonance spectroscopy, for example, NO on molecular sieves [1], NO_2 on copper [2], O_2 on titanium supported surfaces [3], NO on zeolite [4] and nitrogen oxides and oxygen on solid solutions of transition metal ions in oxide matrices [5] have been studied. Unfortunately in all these experiments the surfaces are poorly characterized with respect to surface science standards. UHV *in situ* ESR studies of adsorbates on a clean single-crystal surface were introduced very recently by Baberschke *et al* [6–9].

Introducing ESR to surface science as a new tool promises detailed information about the orientation and dynamics of adsorbates as well as defects in the structure of substrates not as easily accessible with other techniques. Unfortunately there are some problems to deal with. First ESR is not inherently surface sensitive. Preparation of the sample is difficult under these circumstances. Second the signal intensity is directly proportional to the number of available spins (i.e. the number of adsorbed molecules). Considering a monolayer of molecules, the number of spins (about 10^{14}) is close to the detection limit reachable under UHV conditions (the time taken for preparation and measuring is approximately 1 hour). In this sense the present paper will represent some early steps in solving the problems and introducing ESR as a powerful method for the investigation of paramagnetic adsorbates.

On metal surfaces no signal from a paramagnetic species for a monolayer coverage has been observed so far. This is due to the spin exchange of the localized adsorbate spin with the electrons in the conduction band of the metal, which leads to a line broadening, rendering the spectrum unobservable. On the other hand, NO_2 molecules shielded from the surface by a preadsorbed monolayer of rare gas have led to an observable ESR spectrum at submonolayer NO_2 coverage. Baberschke and co-workers [6–9] performed their experiments on NO_2 adsorbates on silver and copper single-crystal surfaces. It is well known, however, that

0953-8984/93/315471+10$07.50

the chemistry of NO_2 on such surfaces at room temperature is rather complicated since several partly dissociately adsorbed NO_2 species exist. Therefore it is reasonable to look for systems with less complex NO_2 adsorption behaviour. As reported by Bartram and Koel [10] TPD and high-resolution electron energy loss (HREEL) spectra show that NO_2/Au(111) chemisorbs non-dissociatively in an upright position. This particular geometry should result in a reduction of the conduction electron density at the nitrogen atom where the unpaired spin is localized and one might speculate that an ESR spectrum could be observed. The larger distance of the nitrogen atom in the adsorption geometry on Au(111) may have this effect.

We will show in this paper that, in spite of the above expectations, NO_2 in the monolayer regime on Au(111) does not show an ESR spectrum. However, there is a very well resolved spectrum of the NO_2 multilayer on Au(111) which is characteristic of a static, random three-dimensionally oriented NO_2 species residing in a N_2O_4 dimer matrix. The temperature dependence of the multilayer signal is investigated.

2. Experimental

Figure 1 shows the combined UHV–ESR apparatus. The chamber is divided into two parts. The upper part is equipped with a combined LEED–AES unit and a QMS to perform structural and chemical analysis of the surface and TPD measurements as well. Here the sample can be prepared by heating with an external filament and sputtering. The lower part of the chamber is constructed from a suprasil finger which is connected via a quartz-to-metal seal to the UHV system and which may be separated from it by a gate valve. The finger is fitted to the inlet of a standard TE_{102} microwave cavity. In its design the apparatus is quite similar to that described in [7]. This configuration allows us to move the sample, mounted on a large travel manipulator into the ESR measuring position without breaking the vacuum (of base pressure better than 1×10^{-10} mbar) after preparation. Cooling of the sample down to 35 K is achieved by a self-designed liquid helium cryostat. After several heating (700–800 °C) and sputtering (2 μA, 600 V, 300 °C) cycles the Auger spectrum of the mechanically polished Au(111) surface revealed no further surface contamination. The LEED pattern indicated that $(22\pm1)x\sqrt{3}$ reconstruction described elsewhere [11, 12]. Adsorption was achieved from the background using NO_2 from a lecture bottle with 99.5% purity. The ESR system is based on a commercial Bruker B-ER 420 spectrometer. We integrated a computer driver for the magnetic field sweep and digital data acquisition in order to use the possibilities of averaging and analysing the spectra. Measuring ESR spectra in the monolayer region requires the sensitivity of the experimental set-up to be tested. By using one particular spectral line of gaseous O_2 we found the sensitivity (i.e. the minimum number of spins detectable) to be 10^{12} spins. Since this technique only gives information concerning the sensitivity over the whole volume of the quartz finger we checked the minimum number of spins detectable by dosing a well defined number of DPPH (2,2-diphenyl-1-picrylhydrazyl) molecules onto a polycrystalline copper slice (5×7 mm^2). The paramagnetic DPPH has been dissolved in benzene and then deposited on the sample. DPPH at room temperature exhibits a spectrum spread only over a limited field range, which is by about a factor ten smaller than with NO_2, the molecule we want to study. Under typical ESR conditions for our NO_2 measurements, however, with a temperature of approximately 30 K, we found the sensitivity to be the same as in the DPPH measurements at room temperature. The sensitivity was found to be better than 10^{13} spins. Thus we are able to detect a paramagnetic monolayer on a single-crystal surface by ESR within a time acceptable for UHV experiments.

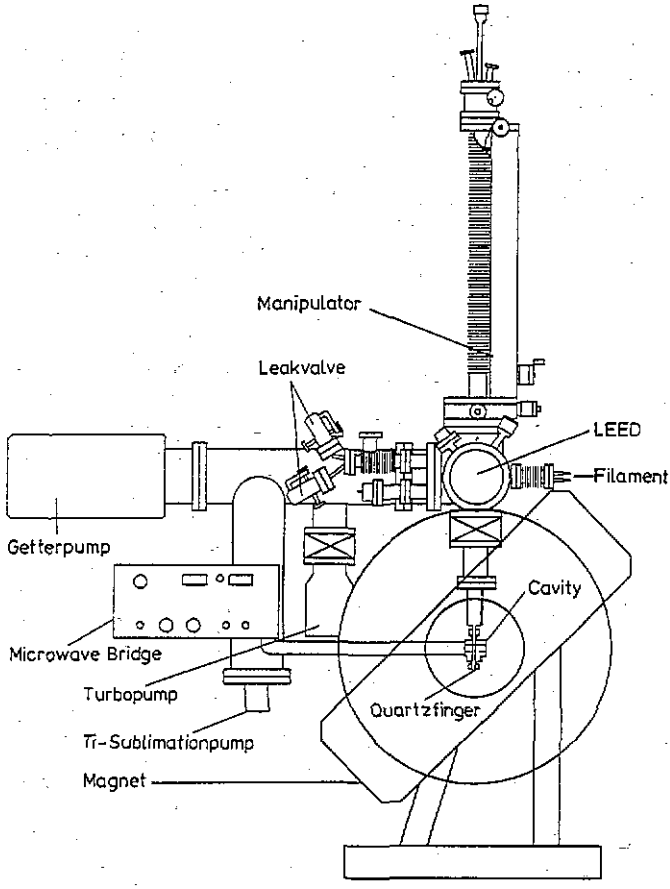

Figure 1. A schematic diagram of a UHV–ESR spectrometer.

3. Results and discussion

As alluded to in the introduction the system NO_2/Au(111) was chosen because it has been thoroughly studied using TPD and HREELS by Koel and his group [10]. Unlike NO_2 adsorption on other coin metals where the chemistry at the surface is not well known, and it is very likely that rather complex reactions take place at the surface, the system NO_2/Au(111) exhibits a very clean and simple adsorption behaviour as revealed by the TPD data shown in figure 2(A). In complete agreement with the work by Bartram and Koel [10] we observe a desorption peak for the monolayer at T = 230 K well separated from a multilayer peak at T = 150 K. Therefore by setting the surface temperature appropriately we can study the monolayer or the multilayer separately. Bartram and Koel [10] have shown via HREELS that in the monolayer regime the NO_2 adsorbs as a molecule and there is no sign of any reaction product. A detailed analysis of the HREEL spectrum reveals that the NO_2 is bound in a surface site of C_{2v} symmetry, with its molecular plane perpendicularly oriented towards the surface plane. It is likely from the work of Bartram and Koel [10] that the molecule is bound with both oxygen atoms, as opposed to the nitrogen atom towards the surface. Whether the bonding mode is bidentate to a single metal atom or to two metal

atoms is not clear at present. In any case the electron spin which couples to the ^{14}N nuclear spin will provide information from an ESR experiment about the involvement of the nitrogen atom in the chemical bond to the substrate. In figure 2(B) the ESR spectra corresponding to the TPD spectra (figure 2(A)) are shown. For the multilayer we clearly observe a rather well resolved solid state spectrum of NO_2 which we shall analyse in more detail later. On the other hand the monolayer shows no ESR signals above the background. This latter result is not completely unexpected because Baberschke and his group had performed a similar experiment on a silver surface without detecting an ESR spectrum. However, since the chemistry of NO_2 on silver is complicated [13], the present result is more clear cut. The explanation given by Baberschke *et al* [6–8] was—and we agree with this interpretation—that the interaction between the electrons at the Fermi energy of the metal substrate and the electron spin on the molecule strongly reduces the average residence time of the electron spin on the molecule. This effect, which is called the Korringa correlation [14], leads to an increase of the line widths resulting in the disappearance of the signal below the background noise. The lines are recovered if the molecules are isolated from the metal surface by an inert gas layer, as was shown by Baberschke and his group [6–8]. The influence of a thin oxide layer as a surface spacer, which we used instead of inert gas layers, is discussed in a separate paper [15]. For a discussion of the NO_2 multilayer ESR spectrum, we may refer to a very detailed discussion by Schaafsma, and co-workers [16–18], who worked out the ESR spectrum of NO_2 in a polycrystalline matrix of N_2O_4. Schaafsma *et al* reported that a condensed N_2O_4 layer as prepared exhibits no ESR spectrum. Only after photochemical initiation did these authors find NO_2 molecules embedded in a N_2O_4 matrix. This is precisely the nature of the multilayer system. Photochemical initiation was not necessary in our preparation.

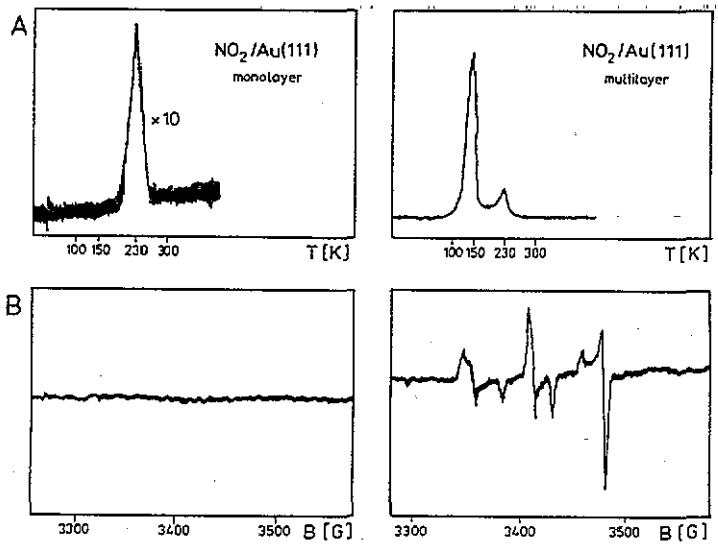

Figure 2. Thermal desorption (TPD) and ESR spectra (T = 35 K) for NO_2/Au(111). (A) TPD signal for monolayer NO_2 coverage (left-hand signal) and one for multilayer coverage (right-hand signal). (B) An ESR spectrum for monolayer NO_2 coverage (left-hand spectrum) and one for multilayer coverage (right-hand spectrum).

Briefly, the NO_2 molecule is in the ground electronic state of $^2A_1$ symmetry. The nuclear spin (I = 1) of the ^{14}N atom leads to a hyperfine triplet. Three-dimensional random

orientation of the NO_2 molecules leads to broad lines for each triplet component. A computer simulation based on a theoretical treatment reported by McClung [19] (see Appendix for details) of such an ESR spectrum is compared with the experimental spectrum in figure 3.

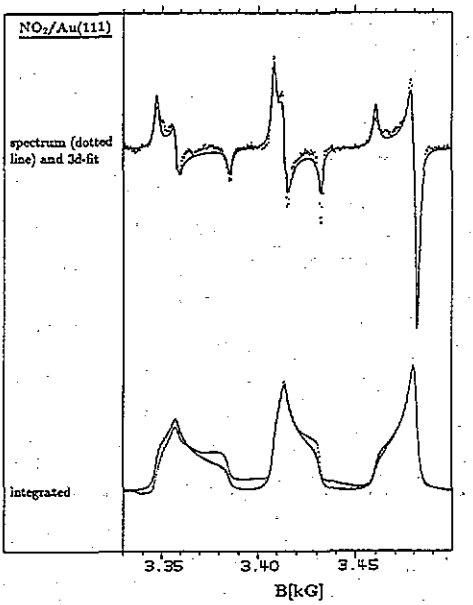

Figure 3. ESR spectra (dotted curves) of multilayer NO_2 on Au(111), taken from figure 2(B) and fitted by a computer simulated three-dimensional random distribution (full curves). The upper spectrum is differentiated and the lower integrated.

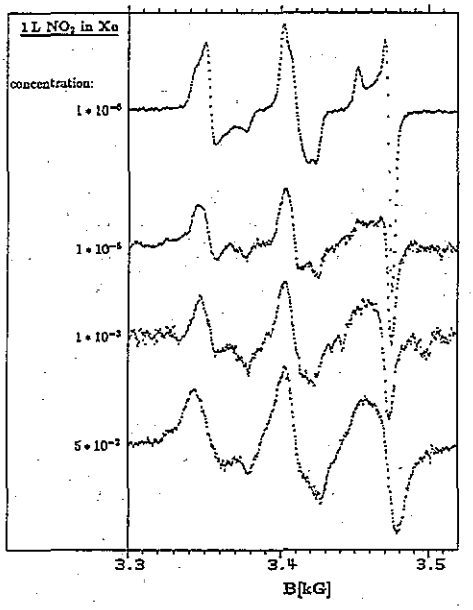

Figure 4. ESR spectra taken of a cocondensed film of xenon and NO_2 (T = 35 K). 1L NO_2 was dosed within a background pressure of xenon. The crudely estimated concentrations are indicated with the spectra.

Both the differentiated as well as the integrated spectra are shown in figure 3. The fit determines g- and A-values and a line width for an individual contributing orientation. The values are collected in table 1 where they can be compared with the literature. The g-value is close to the free-electron value and the A-values are typical for undisturbed NO_2. The line width is in line with non-interacting NO_2 molecules. The effect of diluting the sample on the line width can be seen from figure 4, where NO_2 has been cocondensed with varying amounts of xenon such that the concentration increases by four orders of magnitude. This results in a decrease of the intermolecular distance. It is quite obvious that the line width increases considerably, while the spectrum can still be fitted with a three-dimensional random distribution of the NO_2 molecules. We observe an increase by a factor of three in the line width from 5.7 G to 17.2 G. In figure 5 the line widths as observed in figure 4 are placed in a plot taken from Kittel and Abrahams [27] of the connection between line width and intermolecular distance $\Delta H_{\mathrm{dip}} \sim 1/r^3$ for a model of lattice points populated by identical magnetic dipoles. From this we derive the lower limit for the average intermolecular distance in our sample. This means that the ESR spectrum at the bottom of figure 4 represents an intermolecular distance of 8.2 Å, which may be compared with the NO_2 van der Waals' radius of about 4 Å. For the better resolved NO_2 multilayer spectra (of line width typically 3 G and better) we derive a monomer distance of 14 Å at a minimum. This is an important conclusion for future adsorbate studies. Note, however, that there may

Table 1. Comparison of the g- and A-tensor components for NO_2 in various environments.

system	g-tensor			A-tensor [G]			ref.
gasphase							
NO_2-gas	2.00618	2.00199	1.99102	45.60	66.02	45.20	[20]
matrix isolation							
N_2O_4	2.0054	2.0015	1.9913	50.2	68.3	49.6	[16]
N_2O_4	2.0065	2.0029	1.9960	50.2	68.3	49.6	[21]
Argon(4K)	2.0051	2.0024	1.9914	50.6	63.1	45.4	[22]
Neon(4K)	2.0054	2.0026	1.9919	50.9	63.5	45.9	[23]
adsorption							
Zeolite(Na-X)	2.0043	2.0015	1.9922	51.1	67.5	49.2	[23]
Zeolite(Ca-X)	2.0051	2.0017	1.9921	51	67.6	47.8	[23]
Zeolite(Na-Z)	2.0051	2.0017	1.9913	49.9	65.5	45.9	[24]
ZnO	2.007	2.003	1.994	52.0	64.8	47.3	[25]
MgO	2.005	2.002	1.9915	52.7	67.5	49.1	[26]
Xenon(20K)	2.0045	2.002	1.9915	48.5	64	44.5	[8]
Argon(20K)	2.0055	2.002	1.9915	49	64	45	[8]
Krypton(20K)	2.0055	2.001	1.9915	49	64	45	[8]
NO_2/Au(111)	2.0050	2.0010	1.9912	49.61	66.66	47.31	this work
NO_2/Al_2O_3/NiAl	2.0055	2.0019	1.9920	51.53	66.17	50.08	[15]

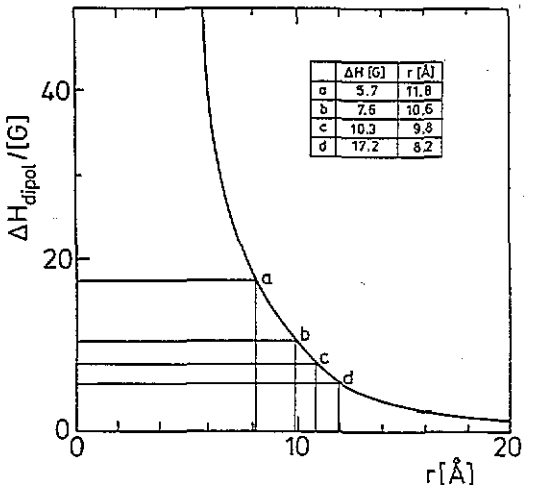

Figure 5. A plot of the intermolecular dipole–dipole interaction as a function of distance [27]. The intermolecular distances deduced from the measured line widths (figure 4) are given in the inset.

be other contributions to the line broadening like the above mentioned Korringa coupling [14] and others that we have not discussed in this paper [28].

An important piece of information, which one might want to extract from spectroscopic data, is the orientation of adsorbed molecules. Usually this is done by angle-dependent measurements. The angle-dependent capabilities of the ESR experiment, where the angle

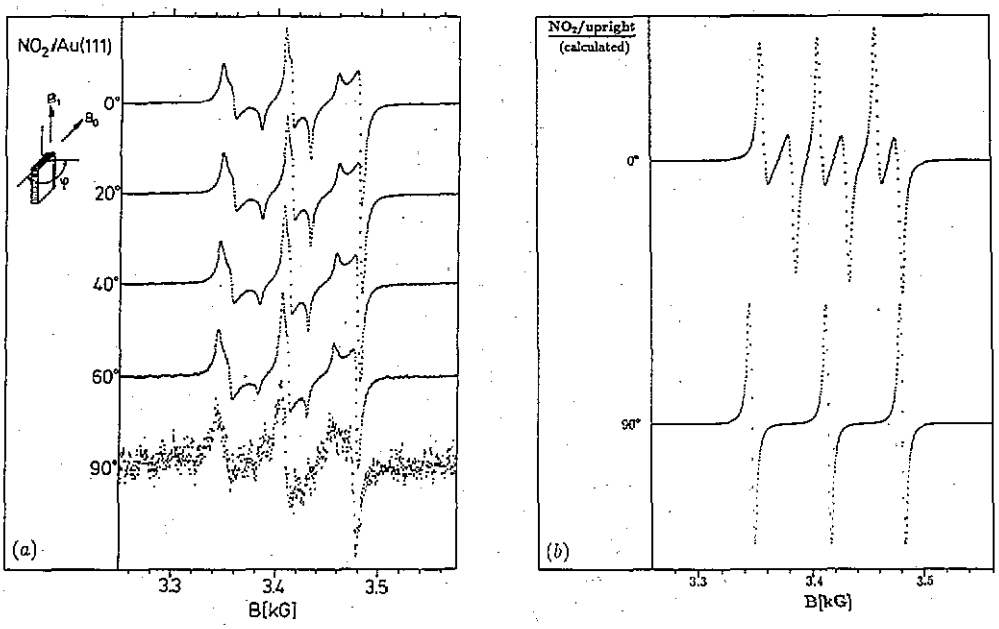

Figure 6. (*a*) ESR spectra of multilayer NO_2 on Au(111) at $T = 35$ K as a function of the angle between the surface and the magnetic field (see inset). (*b*) Simulated line shapes for a monolayer of NO_2 adsorbed, with the C_{2v} axis perpendicular to the surface.

between magnetic field and surface normal can be varied by turning the sample within the cavity, can be demonstrated. Figure 6(*a*) shows a set of angle-dependent spectra of NO_2 on Au(111). There are only small angle-dependent line shape changes observed in this case, in line with the assumption that the distribution is basically three-dimensionally random in the present data. The overall decrease of intensity is caused by the particular microwave field distribution in the cavity relative to the metal single crystal. This effect can be reduced by using a cavity with a cylindrical field distribution, e.g. TE_{011}. In comparison to the measured spectra in figure 6(*a*), figure 6(*b*) shows the expected, i.e. calculated, line shape for NO_2 molecules adsorbed in a geometry as described by Bartram and Koel [10]. The line shape resulting for the upright standing NO_2 molecules (figure 6(*b*)) is strongly angle dependent and may easily be distinguished from the measured spectra which result from a NO_2 layer with randomly oriented molecules. The angular dependence can thus be used to analyse more complex systems where there are oriented species present.

The temperature dependence of the total intensity of the ESR spectrum is shown in the inset in figure 7. The overlayer signal shows a typical Curie behaviour up to the point where desorption starts. A more detailed inspection of the line shapes in the spectra of figure 7 indicates a change in line width. As has been discussed earlier [26] this is likely to be due to translational motion of NO_2 monomers in the physisorbed N_2O_4 film. The exchange between the existing monomers and the surrounding N_2O_4 molecules decreases the relaxation time and this leads to an increase of the line widths. Although the fit (figure 7) between experimental data and computer simulation is rather good there are significant deviations in parts of the spectrum. It is quite likely that these deviations are due to the lack of taking molecular motions into account [3, 17]. The incorporation of molecular dynamics into the simulation is difficult, in particular if the time scale of the motion is comparable to the time scale of the ESR experiment. Calculations are in progress.

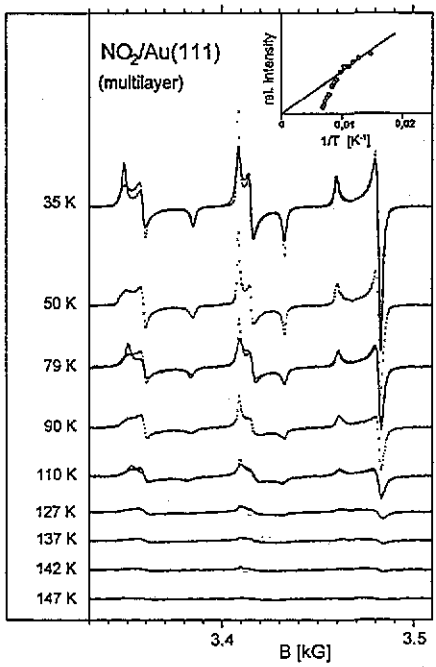

Figure 7. Series of ESR spectra as a function of temperature. For some spectra a fit is included. The temperature dependence of the integrated intensity of the spectra is shown in the inset. The temperature dependence expected from the Curie law is indicated by the full line.

4. Conclusions and outlook

We have recorded ESR spectra of NO_2 adsorbed on a Au(111) surface under UHV conditions. It is the physisorbed multilayer that yields a rather well resolved solid-state ESR spectrum characteristic of isolated NO_2 monomers imbedded in a N_2O_4 dimer matrix. Computer simulation in combination with angle-dependent measurements allows us to demonstrate that the distribution of NO_2 monomers is basically static and three-dimensionally random, i.e. non-oriented. The temperature dependence of the line width indicates exchange between diffusing NO_2 molecules and N_2O_4 dimers in the matrix. TPD allows us to differentiate between the monolayer and multilayer coverage because TPD show clearly separated features for both regimes. By combining TPD with ESR we can unambiguously show that NO_2, which adsorbs and desorbs in the monolayer regime, does not exhibit an ESR spectrum. While it is clear that the study of submonolayer coverages on metal surfaces with ESR spectroscopy is limited we think that for single-crystal oxide surfaces such measurements may be possible, as was recently demonstrated [15].

Appendix. Fitting for static molecules

To fit the experimental data we used the Hamiltonian

$$\boldsymbol{H} = \beta_0 \boldsymbol{S} \boldsymbol{g} \boldsymbol{B} + \hbar \boldsymbol{S} \boldsymbol{A} \boldsymbol{I}$$

for a molecular spin system with electron spin $S = \frac{1}{2}$ and one nuclear spin I. β_0 is the Bohr magneton, g is the g-value tensor, B is the intensity of the applied outer magnetic

field, $\hbar$ is the Planck constant, and A is the tensor of the nuclear–electronic hyperfine interaction. McClung calculated for this Hamiltonian, with the applied magnetic field lying along the laboratory z axis and a sinusoidally varying microwave field of angular frequency ω_0 along the laboratory x axis in second-order time-dependent perturbation theory, the resonance frequencies as a function of the outer magnetic field and the orientation of the paramagnetic molecules relative to the field. In this case the time-dependent perturbation is the microwave field which has to be added to B, leading to a magnetic field vector with components $(B_1(t), 0, B_0)$. The resulting equation for the allowed transitions $|S, M_s\rangle|I, M_I\rangle \rightarrow |S, M_s \pm 1\rangle|I, M_I\rangle$ (M_s and M_I being the quantum numbers of S and I along the z axis) is as follows:

$$\begin{aligned}\hbar\omega_0(B_0, M_I) = {} & g\beta_0 B_0 + \hbar A M_I + (\hbar^2 A_x A_y A_z / 2g\beta_0 B_0 A)[2M_s + 1]M_I \\ & + \{[g_z^2(g^2 A_\alpha^2 - g_\alpha^2 A_z^2)/g_\alpha^2 g^4 A^2] \sin^2\theta \cos^2\theta \\ & + [g_x^2 g_y^2 (A_x^2 - A_y^2)^2 / g_\alpha^2 g^2 A^2] \sin^2\theta \sin^2\phi \cos^2\phi\}(\hbar^2 M_I^2 / 2g\beta_0 B_0) \\ & + \{(g^2 A_\alpha^2 A_z^2 / g_\alpha^2 A^2) + (g_\alpha^2 A_x^2 A_y^2 / g^2 A_\alpha^2) + [g_x^2 g_y^2 g_z^2 A_z^2 (A_x^2 - A_y^2)^2 / g_\alpha^2 g^4 A_\alpha^2 A^2] \\ & \times \cos^2\theta \sin^2\phi \cos^2\phi\}\hbar^2 [I(I+1) - M_I^2] / 4g\beta_0 B_0\end{aligned}$$

$$g_\alpha = (g_x^2 \cos^2\phi + g_y^2 \sin^2\phi)^{1/2}$$

$$g = (g_\alpha^2 \sin^2\theta + g_z^2 \cos^2\theta)^{1/2}$$

$$A_\alpha = (g_x^2 A_x^2 \cos^2\phi + g_y^2 A_y^2 \sin^2\phi)^{1/2} / g$$

$$A = (g^2 A_\alpha^2 \sin^2\theta + g_z^2 A_z^2 \cos^2\theta)^{1/2} / g.$$

For calculating a spectrum under normal ESR conditions (that means sweeping B at a fixed value of the microwave frequency) this formula has to be converted into a formula for $B_0(\omega_0, M_I)$. Multiplication by B_0 leads to a quadratic equation in B_0. The resonant magnetic field then is given by the following:

$$\begin{aligned}B(\omega_0, M_I) = (\hbar / 2g\beta_0) \Big\{ & (\omega_0 - A M_I) - \Big[(\omega_0 - A M_I)^2 - (2A_x A_y A_z / A)[2M_s + 1]M_I \\ & - \{[g_z^2(g^2 A_\alpha^2 - g_\alpha^2 A_z^2)^2 / g_\alpha^2 g^4 A^2] \sin^2\theta \cos^2\theta \\ & + [g_x^2 g_y^2 (A_x^2 - A_y^2)^2 / g_\alpha^2 g^2 A^2] \sin^2\theta \sin^2\phi \cos^2\phi\} 2M_I^2 \\ & - \{(g^2 A_\alpha^2 A_z^2 / g_\alpha^2 A^2) + (g_\alpha^2 A_x^2 A_y^2 / g^2 A_\alpha^2) + [g_x^2 g_y^2 g_z^2 A_z^2 (A_x^2 - A_y^2)^2 / g_\alpha^2 g^4 A_\alpha^2 A^2] \\ & \times \cos^2\theta \sin^2\phi \cos^2\phi\}[I(I+1) - M_I^2] \Big]^{1/2} \Big\}.\end{aligned}$$

To get the principal values of the A tensor in units of the magnetic field (given by McClung in units of angular velocity [19]), the following transformation has to performed:

$$A_i[\mathrm{G}] = \frac{\hbar}{g_i \beta_0} A_i[\mathrm{GHz}] \qquad i = x, y, z.$$

The correctness of this formula is checked by recalculating the microwave frequencies from the calculated resonance field values with those determined via the formula given by McClung [19].

References

[1] Hoffmann B M and Nelson N J 1969 *J. Chem. Phys.* **50** 2598
[2] Nilges M, Shiotani M, Yu C T, Barkley G, Kera Y and Freed J H 1980 *J. Chem. Phys.* **73** 588
[3] Shiotani M, Moro G and Freed J H 1981 *J. Chem. Phys.* **74** 2616
[4] Kasai P H and Gaura R M 1982 *J. Chem. Phys.* **86** 4257
[5] Indovina V, Cordischi D, Febbraro S and Occhiuzzi M 1985 *J. Chem. Soc. Faraday Trans.* I **81** 37
[6] Farle M, Zomack M and Baberschke K 1985 *Surf. Sci.* **160** 205
[7] Zomack M and Baberschke K 1986 *Surf. Sci.* **178** 618
[8] Zomack M and Baberschke K 1987 *Phys. Rev.* B **36** 5756
[9] Baberschke K, Farle M and Zomack M 1987 *Appl. Phys.* A **44** 13
[10] Bartram M E and Koel B E *1989 Surf. Sci.* **213** 137
[11] van Hove M A, Koestner R J, Stair P C, Biberian J P, Kesmodel L L, Bartos I and Somorjai G A 1981 *Surf. Sci.* **103** 189
[12] Perdereau J, Biberian J P and Rhead G E 1974 *J. Phys. F: Met. Phys.* **4** 798
[13] Outka D A, Madix J R, Fisher G B and DiMaggio C 1987 *Surf. Sci.* **179** 1
[14] Korringa J 1950 *Physica* **16** 601
[15] Katter U J, Schlienz H, Beckendorf M and Freund H-J 1992 *Ber. Bunsenges. Phys. Chem.* **97** 340
[16] Schaafsma T J, v.d. Velde G A and Kommandeur J 1967 *Mol. Phys.* **14** 501
[17] Schaafsma T J and Kommandeur J 1967 *Mol. Phys.* **14** 517
[18] Schaafsma T J and Kommandeur J 1967 *Mol. Phys.* **14** 525
[19] McClung R E D 1968 *Can. J. Phys.* **46** 2271
[20] Bird G R, Baird J C, Jache A W, Hodgson J A, Curl R F, Kunkle A C, Brandsford J W, Rastrup-Anderson J and Rosenthal J 1964 *J. Chem. Phys.* **40** 3378
[21] James D W and Marshall R C 1968 *J. Phys. Chem.* **72** 2963
[22] McDowell C A, Nakajima M and Raghunatan P 1970 *Can. J. Chem.* **48** 805
[23] Pietrzak T M and Wood D E 1970 *J. Chem. Phys.* **53** 2454
[24] Shiotani M and Freed J H 1981 *J. Phys. Chem.* **85** 3873
[25] Iyengar R D and Subba Rao V V 1968 *J. Am. Chem. Soc.* **90** 3267
[26] Lunsford J H 1968 *J. Colloid Interface Sci.* **26** 355
[27] Kittel C and Abrahams E 1953 *Phys. Rev.* **90** 238
[28] Zomack M 1987 *Dissertation* Freie Universität Berlin